

Electrospun Immobilized Ruthenium Salen Complex on FeNi₃ Nanofiber for Selective Hydrogenation of Benzene to Cyclohexene

Huang Zhen-xu*, Chen Ling-xia, Ding Yuan-fei, Mao Hai-rong, Gao Hai-rong, Jia Pan-pan

School of Chemistry and Chemical Engineering, Zhengzhou Normal University, Zhengzhou Henan, 450044 China

*E-mail: huangzx1133@163.com huangzx1133@126.com

Received: 8 May 2019 / Accepted: 28 June 2019 / Published: 31 July 2019

FeNi₃ was successfully prepared as a novel magnetic nanoparticles supported ruthenium salen complex (FeNi₃/Ru MNPs). FeNi₃/Ru consigned onto polyvinylalcohol (PVA) utilizing a usual nozzle electrospinning method (PVA/FeNi₃/Ru). The as-collected catalyst is detected using TEM, TGA, XRD, SEM, and VSM. We found that it is an impressive catalyst for selective hydrogenation of benzene to cyclohexene in aqueous solution. Great catalytic activity as well as facility of improvement from the reaction mix along with various reuse times without considerable disadvantages in efficiency were further eco-friendly properties of the catalytic apparatus.

Keywords: Benzene hydrogenation; Cyclohexene; Polyvinyl alcohol; Green chemistry; Ruthenium catalyst

1. INTRODUCTION

Recently, expansion of nanocomposites obtained from electrospun amplified fibrous polymer materials and considering the simulation purposes in academia causes them extremely attractive [1]. There is great potential in the case of Electrospun nanofiber to synthesis the novel polymer nanofibers [2,3]. Moreover, various material selection, adjusted diameter/structure, feasible regulation as well as mass synthesis ability were general benefits of electrospun nano polymers . Mineral nanofibers that have smaller pores as well as higher surface site compared to usual fibers, possess different catalytic usages [3-7]. Notwithstanding massive endeavors assigned to investigate usages of nanofibers obtained by electrospun apparatus, limited tries exist for selecting electrospun nanofibers as amplification for polymer nanohybrids [8,9]. Between whole considered polymers introduced in the lecture, polyvinyl alcohol (PVA) because of its high hydrophilicity low cost and also great chemical persistence is utilized in broad application zones. PVA has been known as a combinatory hydrophilic polymer that can dissolve in water and the polymerization measure or the hydrolysis degree may influence on its

characteristics like, industrial paper usage, emulsificantes, and adhesives [1,10]. Improvement of PVA and also metal oxides, with distinct chemical, thermal, mechanical and stability properties has currently been demonstrated as an impressive path for generating novel materials by particular characteristics and great efficiencies [11-13].

Ruthenium is the most impressive catalyst that used in benzene partial hydrogenation. In this regards, scholars [14] and [15] obtained a cyclohexene production about 2% by Ru catalyst as well as moderators under temperature of 25 °C and pressure of 1 atm into liquid phase hydrogenation of benzene. A crucial stage forward has been constructed and determined an aqueous alkaline solution that including zinc salt along with other additives may significantly enhance the cyclohexene production to ~ 30% [16]. Notwithstanding multiple patents, books and papers on benzene partial hydrogenation [17], impressive catalysts have been proved to ruthenium black and also its alloys. Supported ruthenium catalysts were proved for having cyclohexene productions comparable for the unsupported ones [18–23]. From another point of view, for avoiding association of the unsupported catalysts of ruthenium, powder of zirconia is used into benzene partial hydrogenation. Herein, we report the synthesis of FeNi₃ supported Ru(II) complex (FeNi₃/Ru). Then, nanoparticles of immobilized FeNi₃/Ru with PVA is produced via electrospinning (PVA/FeNi₃/Ru) process. PVA/FeNi₃/Ru used for benzene partial hydrogenation to cyclohexene and after that may be quickly separated by the reaction mixture to be reusing.

2. EXPERIMENTAL

2.1. Materials and Methods

Chemical materials are provided with high purity (Fluka and Merck). Melting phases are found in open capillaries by using an Electrothermal 9100 system were uncorrected. The spectra of FTIR is recorded upon a spectrometer of VERTEX 70 (Bruker) (adjusted in the transmission mode and in spectroscopic grade pellets of KBr for whole considered the powders). Then, morphology is evaluated by transmission electron microscopy (TEM) based on a CM120 Philips Holland transmission electron microscope acting under 120 kV. The phosphorous content within the catalyst is detected by OPTIMA 7300 DV by analyzer of coupled plasma (ICP). Powder X-ray diffraction information is gathered by Bruker D8 Advance model and Cu radiation. The thermogravimetric analysis (TGA) is used based on a NETZSCH STA449F3 under constant heating rate around 10 °C min⁻¹ at the present of N₂. The magnetic evaluations have been performed by using a vibrating sample magnetometer (VSM) under 25 °C temperature. Spectra of NMR is registered at CDCl₃ by utilizing spectrometer of Bruker Avance DRX-400 MHz by TMS that is known as internal standard. The smoothness determination of the yields and reaction analyzing is performed using TLC.

2.2. Approach for the Synthesis of FeNi₃ Nanoparticles

FeCl₂·4H₂O (1.72 g) and NiCl₂·6H₂O (4.72 g) was dissolved within 0.08 L of deaerated extremely cleaned water included in a flask (with three neck) by intense stirring under 800 rpm speed

at the presence of N_2 . When the temperature became $80\text{ }^\circ\text{C}$, 0.01 L of ammonium hydroxide is released (drop by drop), and the reaction is retained for a half hour. The amount of 20 mL (80% concentration) of hydrazine hydrate is released to the upper mentioned suspension. The black yield is then separated with putting the vessel onto a constant magnet as well as the supernatant is added. The obtained black precipitate is washed (six times) for removing the unreacted materials, after that the black yield $FeNi_3$ is exposed to the vacuum [24].

2.3. Approach for the Synthesis of $FeNi_3/SiO_2$ Nanoparticles

At the first, 100 mL of ethanol and 20 mL of distilled water is added to 1 g of magnetic nanoparticles and the obtaining dispersion is sonicated for 600 seconds. After releasing 2.5 mL of ammonia water, 2 mL of tetraethyl orthosilicate is released to the solution. The obtaining dispersion is stirred for 20 h under the temperature of $25\text{ }^\circ\text{C}$, continuously. The magnetic nanoparticles $FeNi_3/SiO_2$ are gathered using magnetic separation and after that washed by ethanol as well as deionized water in sequence [24].

2.4. Approach for the Synthesis of Compound (A) Nanoparticles

For production of (A) MNP, 0.002 mol of $FeNi_3/SiO_2$ MNPs are dispersed within a solution of ethanol (0.008 L), deionized water (0.002 L) and 28 wt % concentrated ammonia aqueous ($NH_3 \cdot H_2O$, 0.0002 L) as well as the addition of 0.002 mol of ethyl3,4-diaminobenzoate. The $FeNi_3/SiO_2$ nanoparticles that have magnetic property are gathered using magnetic separation and, after vigorous stirring for 1 day, washed with ethanol as well as deionized water in sequence [24].

2.5. Approach for the Synthesis of $FeNi_3/SiO_2/Salen$ Nanoparticles

For Synthesis of $FeNi_3/SiO_2/Salen$ MNPs, 4 g of compound (A) is suspended in 0.06 L of toluene solution (0.1 M) of salicylaldehyde and the solution of colloidal is then refluxed for 1 day. The magnetic nanoparticles of $FeNi_3/SiO_2/Salen$ are gathered using magnetic separation and after that washed with ethanol as well as deionized water, sequentially [24].

2.6. Approach for the Synthesis of $FeNi_3/Ru$ Nanoparticles

A 0.5 g $Ru(DMSO)_4Cl_2$, 0.45 g $FeNi_3/SiO_2/Salen$, and 0.8 ml Et_3N in 10 ml methanol is degassed at the presence of nitrogen N_2 as well as refluxed at 4 h. After chilling the room, the precipitate is filtered and then washed with $10\text{ ml} \times 3$ methanol and $10\text{ ml} \times 3$ ether to obtain a specific reddish brown powder. The powder is blended to an excess of 4methylpyridine within 0.5 ml methanol then heated to reflux for around 2 h. The ultimate particle is separated from the solution using a magnetic field and then washed three times (with water) to take any ions available [24].

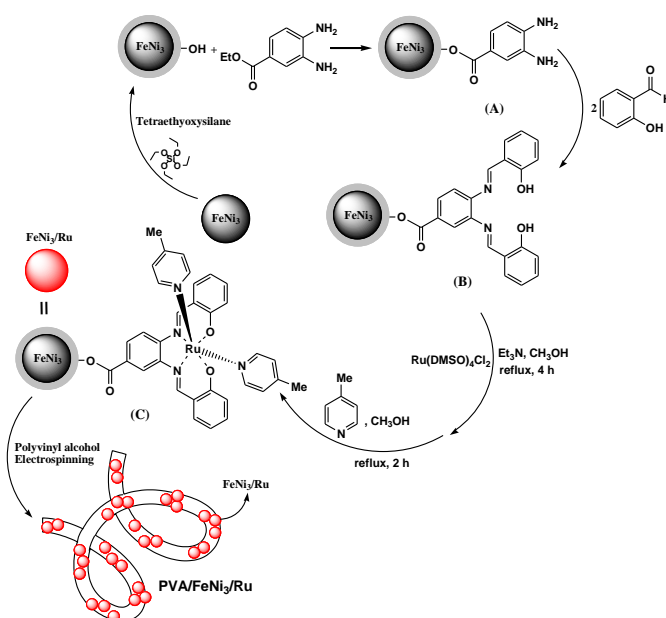
2.7. Approach for the Synthesis of PVA/FeNi₃/Ru MNPs

4 g of FeNi₃/Ru is released in to water (4mL) for 30 min and then is added to PVA (1.6 g) within water (12 mL). The mixture of reaction is irradiated by ultrasound for a half of hour. Provided solution is placed on magnetic stirrer for around 8 hours under the temperature of 80 °C. The electrospinning process for the final provided solution is performed at 25 kV electrical voltage at 25 °C temperature and pressure of 1 atm. The polymer fibers are released utilizing a syringe needle (5ml) by that has outer diameter (OD) of 1.23 mm as well as internal diameter (ID) of 0.83 mm with 0.3 ml/h flow rate. The constructed target is located at 12 cm of the needle tip.

2.8. General procedure for oxidation of phenol

In a reactor made of stainless steel (100 ml volume), a proper H₂ (with pressure of 1.0 MPa) and benzene (10 mmol) are released to a PVA/FeNi₃/Ru MNPs (5 mg) at room temperature. After that, the temperature is increased to temperature of 100 °C using the addition of H₂ that was from a reservoir tank for maintaining a fixed pressure of 2.0 MPa. The remaining H₂ is slowly eliminated. After reaction is occurring, the catalyst is separated by outside magnet also reused to more recycling process. The crude yield mixture is then dried on anhydrous sodium sulphate, and considered to column by utilizing a 6:1 petroleum ether/EtOAc eluent approach onto silica gel for admitting carbonate.

3. RESULTS AND DISCUSSION



Scheme 1. Schematic representation of PVA/FeNi₃/Ru NPs heterostructure preparation.

In this regards the implementation of this aim is the production and functionalization of nanoparticles with magnetic property. The catalyst is provided by sonicating nano-ferrites with salen that works as a potent anchor as well as avoids Ru released in absolute MeOH and then adding

$\text{Ru}(\text{DMSO})_4\text{Cl}_2$ as well as 4methylpyridine. Nanofiber of PVA/ FeNi_3/Ru MNPs is produced by electrospinning process of FeNi_3/Ru according to polyvinyl alcohol that known as a polymer (can be observed in scheme 1).

Moreover, about nanofibrous composite of PVA/ FeNi_3/Ru , the SEM pictures of the pure nanofibers along with various diameters indicated uniform structures as observed in Figure 1b. While it nucleates and develops within the electrospinning method, the FeNi_3/Ru change to the places of the nanofibers of PVA due to its the interior radial direction in the electrostatic area and the fast evaporation about solvents. Actually, Figure 1a indicates the high-resolution picture of TEM for the PVA/ FeNi_3/Ru nanofiber as well as the concise spaces of direct chain separated together. [25] The PVA chains are extended and also self-oriented direction using side along the axis of fiber as well as the straight molecular sections were 150-200 nm long in these chains. Moreover, as seen in Figure 1a, the TEM picture of PVA/ FeNi_3/Ru proven that the atypical white and also gray dots located onto the direct PVA chain that are FeNi_3/Ru . The compression of the FeNi_3/Ru is demonstrated and the mean size of them is computed around 30 nm.

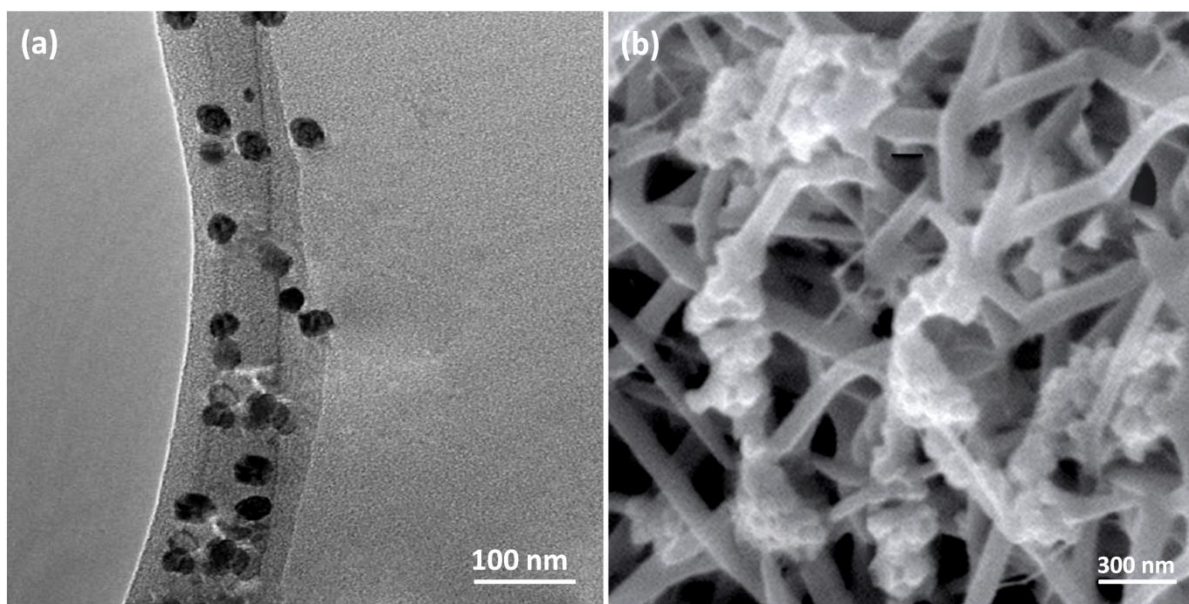


Figure 1. TEM images of a) PVA/ FeNi_3/Ru NPs, and SEM images of b) PVA/ FeNi_3/Ru NPs.

The thermal conduct of PVA/ FeNi_3/Ru MNPs compound nanofiber is examined via thermal gravimetric analysis (as seen in Figure 2). [26] The thermal stability as well as content of organic groups onto the level are determined. The nanofiber of PVA consists of three different bases weight loss steps: (a) until 210 °C near the water evaporation and also volatile composition. (b) We considered second step relating to the polymer chain under temperatures of 230 to 380 °C. (c) At the temperature of 400 °C, the breakage the base chain of PVA is occurred. [27] In term of comparison, the PVA nanofiber sustains total thermal oxidation among 460 and 700 °C, the attendance of PVA/ FeNi_3/Ru MNPs is proven. [28] The residual mass since the polymer dissociation in PVA/ FeNi_3/Ru MNPs was

because of the complex of molybdenum. Based on the TGA figures, the value of transition metal complex within PVA/FeNi₃/Ru MNPs have been predicted to be 18 %.

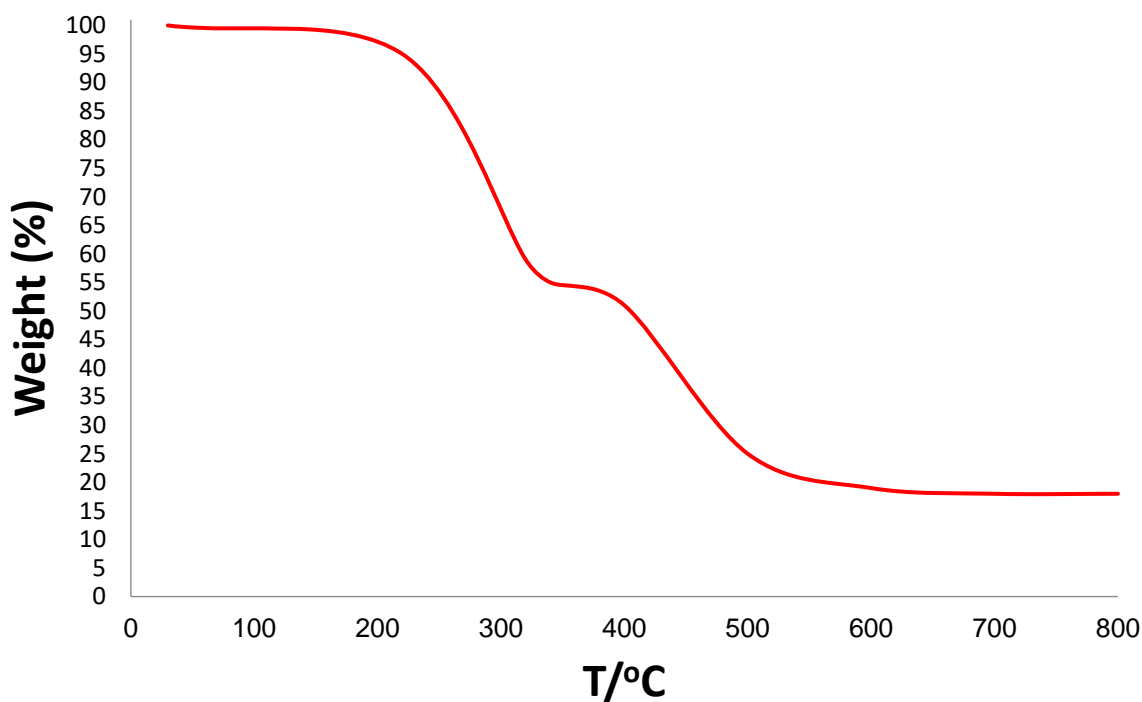


Figure 2. TGA curves of PVA/FeNi₃/Ru composite nanofibrous.

The X-ray diffraction (XRD) figure in the case of FeNi₃, FeNi₃/Ru, and PVA/FeNi₃/Ru MNPs were found in Figure 3. As seen, whole considered samples have the usual diffraction peaks in (220), (311), (400), (422), (511) and (440) that are in proper accord to the information obtained from criterion FeNi₃ sample that is stated by the JCPDS card (No. 19-0629) (Figure 3a). [24] In addition to the iron oxide peak, the XRD schema obtained for FeNi₃/Ru core shell nanoparticles shown a wide featureless peak of XRD for small diffraction angle that is related to exist the amorphous silica (Figure 3b). Figure 3c indicates a usual XRD schema for the PVA/FeNi₃/Ru MNPs. There was no change in it.

Vibrating sample magnetometer (VSM) are utilized or the designation of the nanoparticles magnetic characteristics with the magnetization diagrams of the taken nanocomposite ascribable under the temperature of 300 K. As seen in Figure 3, it is determined that no more magnetism is discovered, so paramagnetic properties are displayed using the nanocomposites. Saturation magnetization amount of 55.3, as well as 10.2 emu/g are calculated for FeNi₃/Ru, and PVA/FeNi₃/Ru MNPs. External magnetic zone along with the ability for quick scattering on removal of magnetic zone is a properties of paramagnetic nano composites by high magnetization amounts. Therefore, the resultant nanocomposite represented proper magnetic responsivity proposing potential usage for targeting as well as separation.

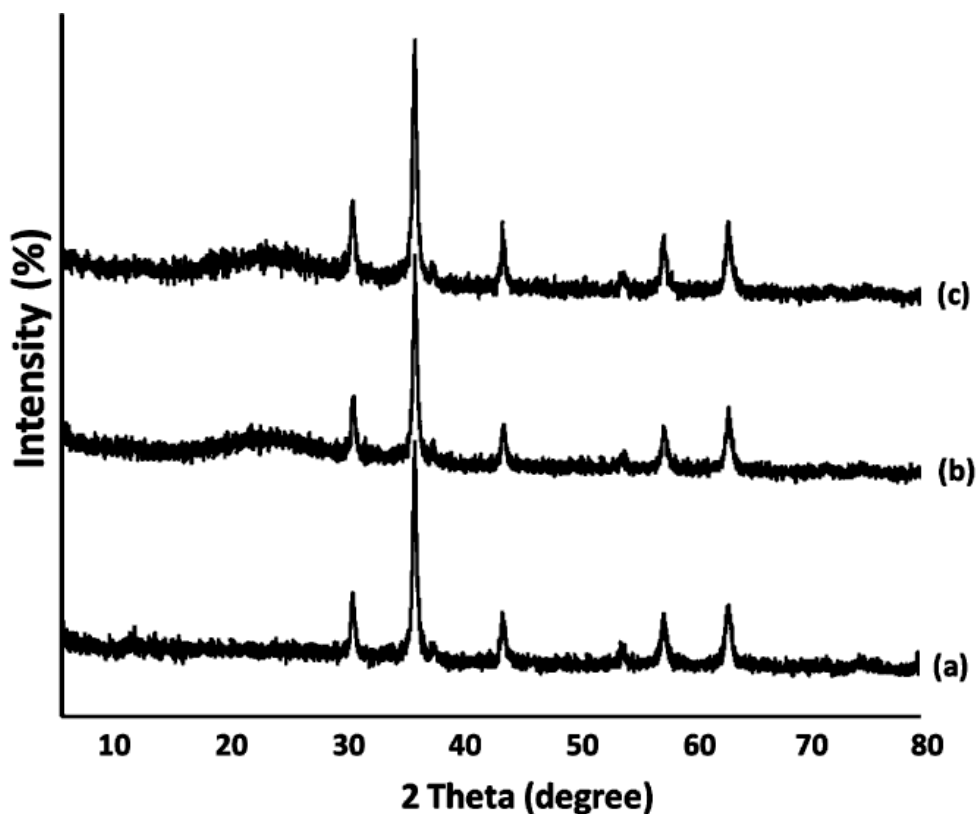


Figure 3. XRD analysis of (a) FeNi₃, (b) FeNi₃/Ru, and (c) PVA/FeNi₃/Ru MNPs.

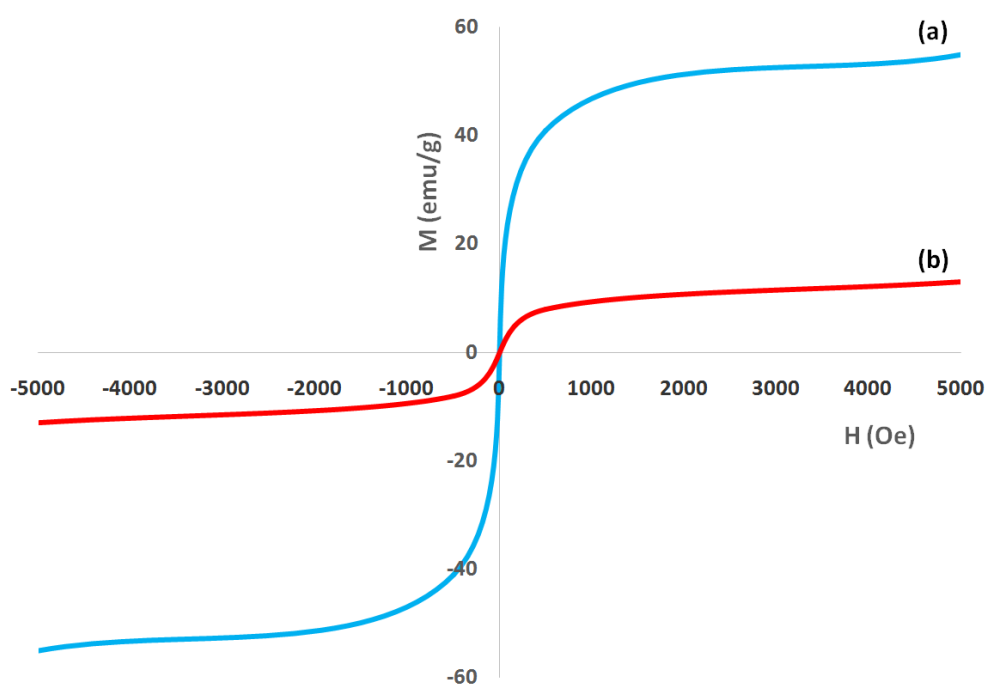


Figure 4. Room-temperature magnetization curves of (a) FeNi₃/Ru, and (b) PVA/FeNi₃/Ru.

For improving the benzene hydrogenation with cyclohexene in the attendance of PVA/FeNi₃/Ru MNPs, as a catalyst, is used as a base approach. The effect of different factors like solvent, and time (as seen in Table 1) are investigated as the model of reaction. The influence of

solvents upon the reaction is tested (referred to Table 1, Entries 1–15). Based on analyzed outcomes of solvents, while polar protic solvents, like ethanol, isopropanol, methanol, and water are illustrated that any value of the favorable product is not created. Never the less, the cross-coupling output yield is mean in its polar aprotic solvents, like EtOAc, CHCl₃, DMF and CH₂Cl₂ as well as DMSO. While the reaction is performed in less polar solvents, like even toluene or anisole, proper for high carbonylative cross-coupling products are separated. [29] Never the less, the carbonylative cross-coupling yield was achieved in low product in polar solvents. In the present work, it is determined that common heating for solvent free was more impressive compared to utilizing solvents (referred to Table 1, Entries 16). In the optimized states, the reaction advance in the case of the shortest time essential in the attendance of 5 mg of PVA/FeNi₃/Ru MNPs was determined using GC apparatus, which appropriate products of synthesis of cyclohexene be obtained in 40 min (referred to Table 1, Entries 17).

Table 1. Hydrogenation of benzene to cyclohexene by PVA/FeNi₃/Ru MNPs in different solvents and time.^a

Entry	Solvent	Time (min)	Yield (%) ^b
1	EtOH	60	-
2	MeOH	60	-
3	<i>i</i> -PrOH	60	-
4	H ₂ O	60	-
5	CH ₃ CN	60	23
6	DMF	60	8
7	CH ₂ Cl ₂	60	13
8	CHCl ₃	60	7
9	EtOAc	60	10
10	THF	60	12
11	Toluene	60	23
12	<i>n</i> -Hexane	60	-
13	Dioxane	60	-
14	DMSO	60	9
15	Anisole	60	26
16	solvent-free	60	67
17	solvent-free	50	67
18	solvent-free	40	67
19	solvent-free	30	43

^a Reaction conditions: appropriate H₂ (2 MPa), benzene (10 mmol), and PVA/FeNi₃/Ru MNPs (5 mg), at 100 °C.

^b Isolated yields.

For enhancing reaction states for PVA/FeNi₃/Ru MNPs catalyst, the influences of different reaction factors are studied. Figure 5 shows the effect of temperature on this reaction. As seen, the cyclohexene yield enhanced to 67 % under 100 °C temperature and at 20 bar H₂ pressure over 40 min. Whilst more enhance in the temperature caused in a slight reduce in the product yield because of

producing a small quantity of some by products, like the propylene oxide isomerization. [30] Accordingly, the optimized temperature for this reaction was around the temperature of 100 °C. The pressure of H₂ has a dramatic effect on the hydrogenation reaction. The reaction rate is quickly increased in the pressure range from 1.8 to 2.0 MPa as illustrated in Figure 6. Never the less, the product reduced while the pressure obtained 2.4 MPa. According to these works, it may be concluded that enhancing reaction pressure was favorable to generate cyclohexene [31] while the reaction pressure was under pressure of 2.4 MPa. Accordantly, the H₂ pressure around 2.0 MPa is considered as proper state.

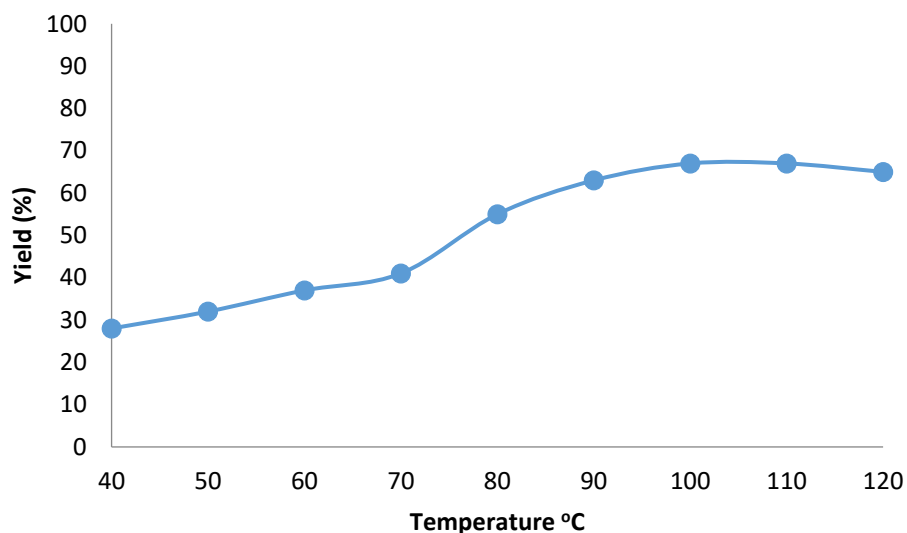


Figure 5. Effect of temperature on yield of hydrogenation of benzene to cyclohexene.

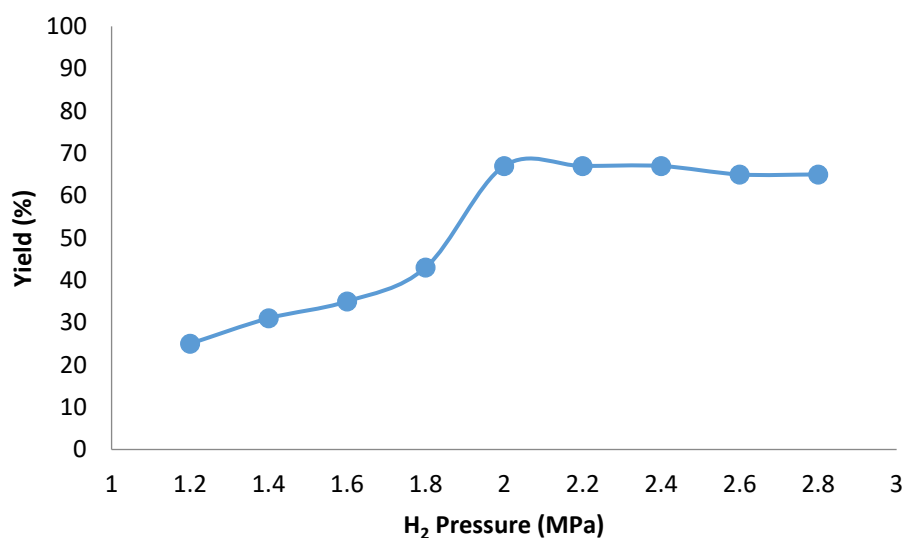


Figure 6. Effect of H₂ pressure on the hydrogenation of benzene to cyclohexene.

To show its uniqueness, novelty, and to further evaluate the present method, the catalytic activities of the PVA/FeNi₃/Ru were compared with those of the reported Co-catalyzed hydrogenation

of benzene to cyclohexene in terms of the yield, temperature, and H₂ pressure. This reaction was obviously superior to the most supported Ir, Rh, or Pt catalysts. [32-38] Also, our catalyst shows a better catalytic activity in comparison with iridium nanoparticles on zeolite unsupported and Ir-NPs in solvent-free conditions or ionic liquid dispersions. PVA/FeNi₃/Ru MNPs is a more versatile approach for hydrogenation reactions of benzene to cyclohexane in terms of energy consumption, time consumption, lower H₂ pressure, catalyst preparation, and in eco- and economic friendly aspects (Table 2).

Table 2. Hydrogenation reactions of benzene to cyclohexane by different catalysts.

Entry	Catalyst	p H ₂ (bar)	T (°C)	TOF (h ⁻¹)	Reference
1	PVA/FeNi ₃ /Ru	2.0	100	11000	This work
2	Ir@zeolite	3.0	25	3190	32
3	Rh@CNTs	10.0	25	2414	35
4	Ir-NP/IL	4.0	75	85	33
5	Ru/SiO ₂	20.0	100	5000	34
6	Ir-NPs	4.0	75	71	33
7	Pt-NP//IL	4.0	75	11	38
8	Rh/AlO(OH)	4.0	75	1700	37
9	Pt-NPs	4.0	75	28	38
10	Rh@TRGO	4.0	50	310	36

In order to determine the effect of reaction alone, a set of experiments were performed in selected conditions including initial PVA/FeNi₃/Ru nano-composite of 1 mg, 10 mmol of benzene, and H₂ pressure 2.0 MPa. Figure 7 shows the obtained results. Removal performance around 11 % showed that the effect of adsorption is entirely low. Moreover, the effect of plain FeNi₃/Ru in optimized states without PVA has been compared to PVA/FeNi₃/Ru nanocomposite. According to yield of 51 %, it can be concluded that PVA increased the removal dramatically. The synergistic impact of PVA in comparison with plain PVA/FeNi₃/Ru in reaction is likely first because of cleaning the electrons by taking into account of PVAs in the compound, which allows the separation of electron holes. [39, 40] Moreover, we found that PVA performs as a photo-sensitizer. [41]

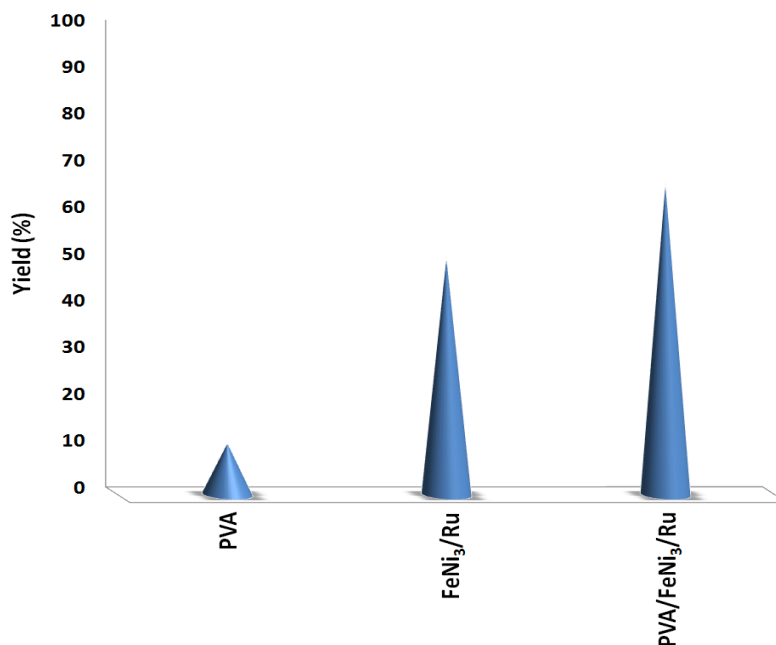


Figure 7. Comparison the hydrogenation of benzene to cyclohexene between catalytic through PVA, catalytic with plain FeNi₃/Ru and catalytic with PVA/FeNi₃/Ru in the same conditions.

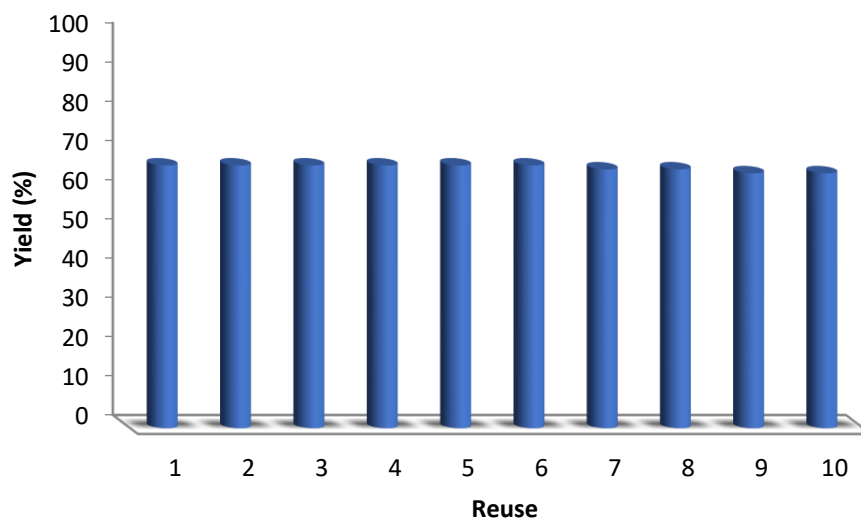


Figure 8. Reuses performance of the catalysts.

In addition, the rather significant studies concerning the recovery and utilization of the catalyst of the PVA/FeNi₃/Ru MNPs are done (as seen in Figure 7). The activity of this catalysis are analyzed using the production of this reaction at the optimized states. For any step, the catalyst is isolated from the reaction mixture, and immediately reutilized for further reaction at the optimal reaction states. As can be seen in figure 7, it is clear that the catalyst would be reutilized for around ten times and no considerable drop in the production of cyclohexene, showing high consistency of PVA/FeNi₃/Ru MNPs catalysis. The synergistic effect of PVA compared to plain DFNT/Ni in cycloaddition reaction is probably first due to scavenging the electrons by PVA in the composite that facilitates the separation

of electron holes. In addition, it is believed that PVA acts as a photo-sensitizer. In addition, the value of ruthenium leached within the solution for hydrogenation of benzene to cyclohexene after each run is evaluated using ICP. The catalyst indicated very little leaching in each turn that 0.5 % metal leaching discovered after the ten run, so showing its consistency at the reaction states as illustrated in Figure 9.

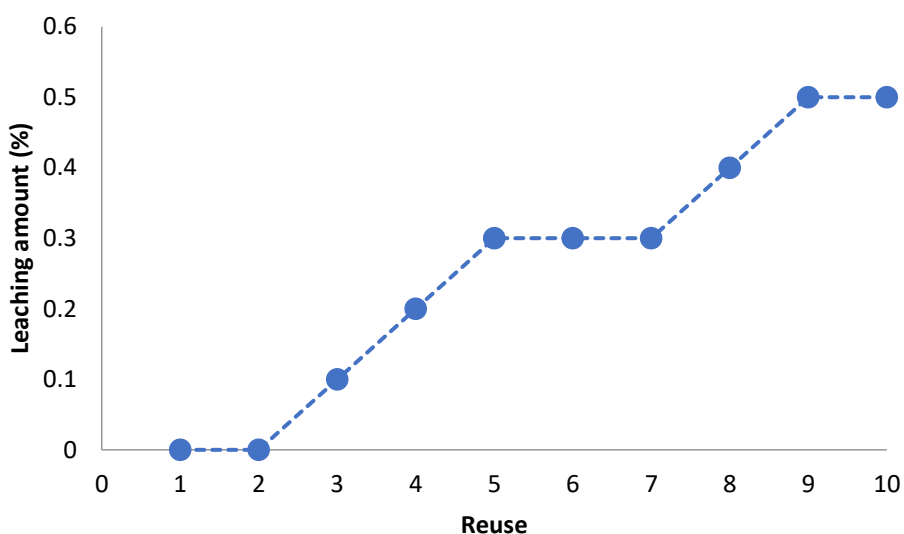


Figure 9. Recyclability of the catalyst for hydrogenation of benzene to cyclohexene.

In addition, a complete study is performed to clarify the catalyst heterogeneous nature. Firstly, we done the hot filtration experiment on to the hydrogenation of benzene to cyclohexene at premium states and determined that the catalyst is magnetically deleted in situ after around 32% for 20 min removal. In addition, the reactants are permissible to tolerate more reaction. The outcomes demonstrated that, after removing the heterogeneous catalyst, the free catalyst remnant is feeble active, and the conversion about 34% is obtained after 40 min of the hydrogenation of benzene to cyclohexene. It proved that the catalyst worked heterogeneously during the reaction and resulted just slight leaching done in the reaction. Secondly, for ensuring the heterogeneous pattern of the catalyst, the mercury poisoning examine is additionally performed. Mercury (0) is imbibed as a metal or using synthesis and dramatically deactivated the metal catalyst on active surface and so tranquilized the catalyst activity. Conducted experiment is proof of the heterogeneous catalyst. This test has been performed with the aforesaid model of reaction under optimal states. [42] After 20 min of the reaction, about 300 molar mercury is released to the reaction compound. The reaction zone is stirred for above 40 min. In this reaction, no further conversion is seen after 20 min from the catalyst being poisoned. A kinetics scheme of the reaction under the attendance of Hg(0) is demonstrated in Figure 10. The negative outcomes obtained from the whole heterogeneity experiments (Hg(0) poisoning as well as hot filtration) proposed that the solid catalyst is really heterogeneous and no acquirable ruthenium leaching performed upon hydrogenation of benzene to cyclohexene. The TEM picture indicated that the a generic white and gray dots placed on the straight chain of PVA were FeNi₃/Ru MNPs after the 10th run (refer to Figure 11a). Noted that the nanocatalyst has not indicated any morphological variations

that is proved by the FE-SEM pictures, which captured from the recovered catalyst (reffer to Figure 11b).

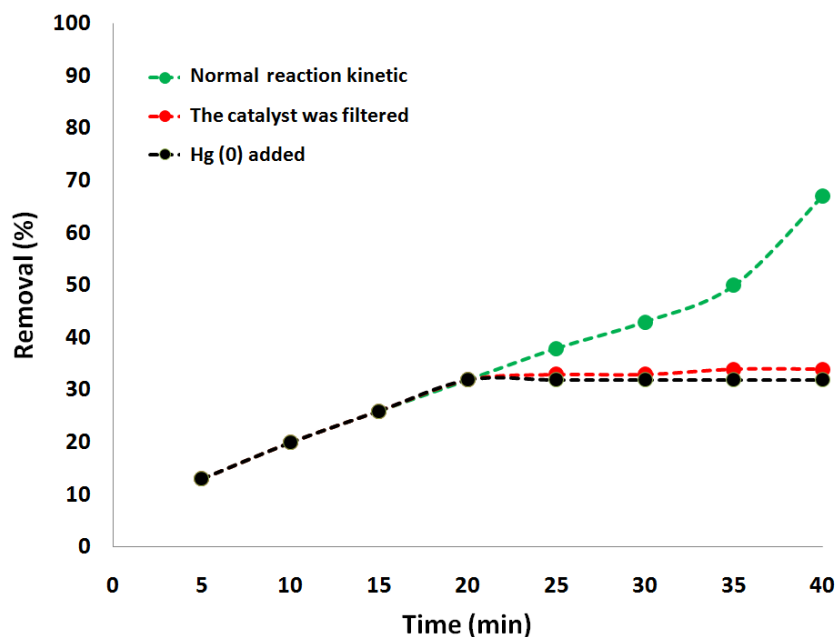


Figure 10. Reaction kinetics, Hg(0) poisoning, and hot filtration studies for hydrogenation of benzene to cyclohexene.

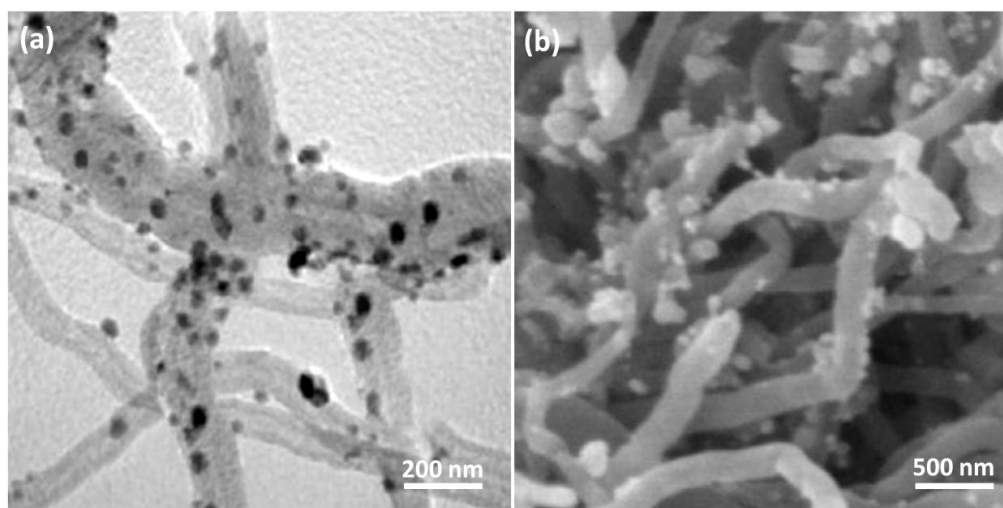


Figure 11. (a) TEM, and (f) FE-SEM images of the recovered PVA/FeNi₃/Ru MNPs after the 10th run for hydrogenation of benzene to cyclohexene.

4. CONCLUSIONS

From above discussion, we have found that FeNi₃ nanoparticles was prepared from FeCl₂•4H₂O and NiCl₂•6H₂O. in addition, an electrospun nanofiber is produced by one new ruthenium salen complex base on natural FeNi₃ nanoparticles. PVA/FeNi₃/Ru MNPs used as a catalyst for hydrogenation of benzene to cyclohexene under solvent-free condition. PVA/FeNi₃/Ru MNPs

indicated outstanding properties such as abundance of strong active sites, great mechanical and thermal stability and high surface area. High surface zone because of the attendance of dendrimeric wall-like fibrous nanostructure as well as respective channels has constructed this fibrous PVA/FeNi₃/Ru MNPs that can open up wide better opportunities for usage in various scientist fields.

ACKNOWLEDGEMENT

The Key Scientific Research Projects of Henan Province Colleges and Universities(No. 19B150021)

References

1. M. North, R. Pasquale, C. Young, *Green Chem.*, 12 (2010) 1514.
2. K. Soga, Y. Tazuke, S. Hosoda, S. Ikeda, *J. Polym. Sci. Polym. Chem. Ed.*, 15 (1977) 219.
3. B. Ochiai, E.T. Prog, *Polym. Sci.*, 30 (2005) 183.
4. S.F.Tang, D.L.Yuan, Y. D. Rao, M.H. Li, G.M.Shi,J.M. Gu, T.H.Zhang, *J Hazard. Mater.*, 366(2019)669.
5. P. H. Shao, J. Y. Tian, F. Yang, X. G. Duan, S. S. Gao, W. X. Shi, X. B. Luo, F. Y. Cui, S. L. Luo and S. B. Wang, *Adv. Funct. Mater.*, 28 (2018) 1705295.
6. L.M. Yang, Z.L. Chen, D. Cui, X. B. Luo, B. Liang, L.X. Yang, T. Liu, A. J. Wang and S. L. Luo. *Chem. Eng. J.*, 359(2019)894.
7. Q.Zhang,S.Bolisetty,Y.Cao,S.Handschin, J. Adamcik, Q.Peng, R.Mezzenga, *Angew .Chem. Int. Edit .*, 58(2019) 6012.
8. A. Baba, T. Nozaki, H. Matsuda, *Bull. Chem. Soc. Jpn.*, 60 (1987) 1552.
9. A.A.G. Shaikh, S. Sivaram, *Chem. Rev.*, 96 (1996) 951.
10. M. North, R. Pasquale, *Angew. Chem. Int. Edit.*, 48 (2009) 2946.
11. P. Yan, H.W. Jing, *Adv. Synth. Catal.*, 351 (2009) 1325.
12. L. Jin, Y. Huang, H. Jing, T. Chang, P. Yan, *Tetrahedron: Asymmetry*, 19 (2008) 1947.
13. R.L. Paddock, S.T. Nguyen, *Chem. Commun.*,21 (2004) 1622.
14. F. Hartog, *J. Catal.*, 2 (1963) 79.
15. F. Hartog, J.H. Tebben, *Proc. Int. Congr. Catal.*, 2 (1965) 1210.
16. S.M. Sadeghzadeh, *RSC Advances.*, 5 (2015) 68947.
17. J. Struijk, M. d'Angremond, W.J.M. Lucas-de Regt, J.J.F. Scholten, *Appl. Catal. A.*, 83 (1992) 263.
18. G.B.Zhou, J.L.Liu, X.H.Tan, *Ind Eng Chem Res.*, 1209111(2012)3583.
19. S. Niwa, F. Mizukami, T. Tsuchiya, K. Shimizu, S. Imai, J. Imamura, *J. Mol. Catal.*, 34 (1986) 247.
20. S.C. Hu, Y.W. Chen, *Ind. Eng. Chem. Res.*, 40 (2001) 6099.
21. S.C. Hu, Y.W. Chen, *J. Chem. Technol. Biotechnol.*, 76 (2001) 954.
22. S.H. Xie, M.H. Qiao, H.X. Li, W.J. Wang, J.F. Deng, *Appl. Catal. A.*, 176 (1999) 129.
23. Z. Liu, S.H. Xie, B. Liu, J.F. Deng, *New J. Chem.*, 23 (1999) 1057.
24. S.M. Sadeghzadeh, *Catal Lett .*, 146 (2016) 2555.
25. X. Liu, J. Ma, X. Wu, L. Lin, X. Wang, *ACS Nano*, 11 (2017) 1901.
26. S. Yang, P. Lei, Y. Shan, D. Zhang, *Appl. Surf. Sci.*, 435 (2018) 832.
27. K.C.S. Figueiredo, T.L.M. Alves, C.P. Borges, *Braz. J. Chem. Eng.*, 31 (2014) 747.
28. A.K. Sahu, G. Selvarani, S. Pitchumani, P. Sridhar, A.K. Shukla, N. Narayanan, A. Banerjee, N. Chandrakumar, *J. Electrochem. Soc.*, 155 (2008) 686.
29. S.M. Sadeghzadeh, *Green Chem.*, 17 (2015) 3059.
30. H. Liu, S. Liang, W. Wang, T. Jiang, B. Han, *J. Mol. Catal. A: Chem.*, 341 (2011) 35.

31. R.M. Esteban, K. Schütte, P. Brandt, D. Marquardt, H. Meyera, F. Beckert, R. Mülhaupt, H. Kölling, C. Janiak, *Nano-Structures & Nano-Objects*, 2 (2015) 11.
32. Y. Tonbul, M. Zahmakiran, S. Ozkar, *Appl. Catal. B: Environmental.*, 148-149 (2014) 466.
33. G.S. Fonseca, A.P. Umpierre, P.F.P. Fichtner, S.R. Teixeira, J. Dupont, *Chem. Eur. J.*, 9 (2003) 3263.
34. X. Kang, J. Zhang, W. Shang, T. Wu, P. Zhang, B. Han, Z. Wu, G. Mo, X. Xing, *J. Am. Chem. Soc.*, 136 (2014) 3768.
35. H.-B. Pan, C.M. Wai, *J. Phys. Chem. C.*, 113 (2009) 19782.
36. D. Marquardt, C. Vollmer, R. Thomann, P. Steurer, R. Mülhaupt, E. Redel, C. Janiak, *Carbon*, 49 (2011) 1326.
37. I.-S. Park, M.S. Kwon, K.Y. Kang, J.S. Lee, J. Parka, *Adv. Synth. Catal.*, 349 (2007) 2039.
38. C.W. Scheeren, G. Machado, J. Dupont, P.F.P. Fichtner, S.R. Texeira, *Inorg. Chem.*, 42 (2003) 4738.
39. G. Mbambisa, K.M. Molapo, C.E. Sunday, C. Arendse, P. Baker, E. Iwuoha, *Int. J. Electrochem. Sci.*, 11 (2016) 9734.
40. L. Fan, J. Chen, G. Qin, L. Wang, X. Hu, Z. Shen, *Int. J. Electrochem. Sci.*, 12 (2017) 5142.
41. M.H. Hussin, N.A. Husin, I. Bello, N. Othman, M.A. Bakar, M.K.M. Haafiz, *Int. J. Electrochem. Sci.*, 13 (2018) 3356.
42. M. Argyle and C. Bartholomew, *Catalysts*, 5 (2015) 145.

© 2019 The Authors. Published by ESG (www.electrochemsci.org). This article is an open access article distributed under the terms and conditions of the Creative Commons Attribution license (<http://creativecommons.org/licenses/by/4.0/>).